Supplementary data

Exploration of the Supramolecular Interactions Involving Tris-Dipicolinate Lanthanide Complexes in Protein Crystals by a Combined Biostructural, Computational and NMR study

Elise Dumont,[a] Guillaume Pompidor,[†b] Anthony D'Aléo,[‡ a] Jean Vicat,[b] Loïc Toupet,[c] Richard Kahn,[b] Eric Girard,[b] Olivier Maury,*[a] and Nicolas Giraud*[d]

[a] Laboratoire de Chimie, UMR 5182 CNRS – ENS-Lyon, 46 allée d'Italie, 69364 Lyon cedex 07, France,
[b] Institut de Biologie Structurale J.-P. Ebel UMR 5075 CEA-CNRS-UJF-PSB, 41 rue Jules Horowitz, 38027 Grenoble cedex 1, France,
[c] Groupe de la Matière Condensée et Matériaux, UMR 6626 CNRS-Université de Rennes 1, Campus de Beaulieu, 35042 Rennes cedex, France,
[d] Laboratoire de RMN en milieu orienté, ICMMO, UMR 8182 CNRS Université Paris-Sud, bât 410, 91405 Orsay cedex, France

* E-mail: *olivier.maury@ens-lyon.fr*, *nicolas.giraud@u-psud.fr*

Table of Content

Experimental section

[EtGua]$_3$[Tb(DPA)$_3$].2H$_2$O. In a 50 mL round bottom flask, [Cs]$_3$[Tb(DPA)$_3$].7H$_2$O (500 mg, 0.43 mmol) was dissolved in 25 mL of water and ethylguanidine hydrochloride (530 mg, 21.5 mmol) was added. The desired product was isolated as colorless crystals by slow evaporation over one week (112 mg, 28 % yield). ^{1}H-NMR (200.13 MHz, D$_2$O, [C]= 21.2 x 10^{-3} mol.L^{-1}): 39.57 ppm (b, 2H), 35.53 ppm (b, 1H), 1.59 ppm (bs, 6H), 0.305 ppm (bs, 9H); ^{13}C-NMR (50.332 MHz, D$_2$O): 307.58, 232.80, 179.94, 150,14, 88.85, 34.30, 11,81. Elemental Analysis: Calcd for C$_{30}$H$_{39}$N$_{12}$O$_{12}$Tb.2H$_2$O: C, 37.74; H, 4.54; N, 17.61; Found: C, 37.44; H, 4.49; N, 17.38.

[EtNH$_3$]$_3$[Tb(DPA)$_3$].2H$_2$O. In a 50 mL round bottom flask, 2,6-Pyridinedicarboxylic acid (1.00 g, 6.0 mmol) and ethylamine (405 mg, 9.0 mmol) were suspended in water (10 mL) and stirred until everything dissolved. TbCl$_3$. 6H$_2$O (745 mg, 2.0 mmol) were added to the solution. The solution was stirred at room temperature for 1hour. The solution was reduced to 5 mL and the remaining water solution was stored at 4°C for four nights (175 mg, 11 % yield). ^{1}H-NMR (200.13 MHz, D$_2$O, [C]= 35.6 x 10^{-3} mol.L^{-1}): 39.35 (b, 2H), 35.33 (b, 1H), 1.08 (bs, 6H), 0.36 (bs, 9H); ^{13}C-NMR (50.332 MHz, D$_2$O): 308.63, 233.17, 180.11, 88.60, 33.10, 11.20; Elemental Analysis: Calcd for C$_{27}$H$_{33}$N$_6$O$_{12}$Tb.2H$_2$O: C, 39.14; H, 4.50; N, 10.14; Found: C, 39.52; H, 4.63; N, 9.88.

[Imz]$_3$[Tb(DPA)$_3$].2H$_2$O. In a 50 mL round bottom flask, 2,6-Pyridinedicarboxylic acid (1.00 g, 6.0 mmol) and imidazole (613 mg, 9.0 mmol) were suspended in water (10 mL) and stirred until everything dissolved. TbCl$_3$. 6H$_2$O (745 mg, 2.0 mmol) were added to the solution. The solution was stirred at room temperature for 1hour. The solution was reduced to 5 mL and the remaining water solution was stored at 4°C for one night (968 mg, 56 % yield). ^{1}H-NMR (200.13 MHz, D$_2$O, [C]= 19.7 x 10^{-3} mol.L^{-1}): 39.41 (b, 2H), 35.38 (b, 1H), 5.76 (bs, 6H), 4.00 (bs, 3H); ^{13}C-NMR (50.332 MHz, D$_2$O): 307.61, 234.03, 180.86, 130.54, 117.25, 88.77; Elemental Analysis: Calculated for C$_{30}$H$_{39}$N$_{12}$O$_{12}$Tb.2H$_2$O: C, 37.74; H, 4.54; N, 17.61; Found: C, 37.44; H, 4.49; N, 17.38.

Copyright The Royal Society of Chemistry, 2013

Table S1. Crystals data and refinement parameters for $[A^M]_3[Tb(DPA)_3]$

A^M	EtGua	EtNH₃	Imz
Formula	$2(TbC_{21}H_9O_{12}N_3), 6(C_2H_5NH_3), 6 H_2O$	$TbC_{21}H_9O_{13}N_3, 3(C_3H_{10}N_3), 2 H_2O$	$TbC_{21}H_9O_{12}N_3, 3(C_3H_5N_2), 3 H_2O$
M / g	1693.12	954.68	915.55
Size / mm³	0.25*0.25*0.12	0.30*0.30*0.25	0.18*0.18*0.06
Systems	Triclinic	Triclinic	Triclinic
Space group	P-1	P-1	P-1
a / Å	9.4638(6)	11.4612(4)	10.9482(2)
b / Å	17.9275(9)	12.1930(3)	12.0839(2)
c / Å	20.2353(9)	14.0695(5)	13.9323(3)
α / deg	77.405(7)	85.682(2)	89.007(3)
β / deg	81.990(8)	78.211(2)	85.655(2)
γ / deg	84.189(7)	80.168(2)	67.354(3)
V / Å³	33.08.9(3)	1894.8(1)	1696.06(1)
Z	2	2	2
λ(Mo/Kα) / Å	0.71073	0.71073	0.71073
F(000)	1712	968	916
T / K	100(1)	120(1)	120(1)
Dc / g.cm⁻³	1.699	1.673	1.793
θ range / deg	2.74 - 27.00	2.96 - 27.00	2.93 - 28.00
hkl ranges	-12,12 -22,21 -25,25	0,14 -15,15 -17,17	-14,14 -15,15 -17,17
Variable	883	514	515
Refln measured	13197	7999	7376
Refln I> 2σ(I)	11033	7586	7084
R1 I> 2σ(I)	0.0257	0.0194	0.0183
R1 all data	0.0349	0.0213	0.0202
ωR2 I> 2σ(I)	0.0645	0.0500	0.0481
ωR2 all data	0.0674	0.0519	0.0491

Copyright The Royal Society of Chemistry, 2013

Theoretical simulations

DFT calculation details.

Static calculations were performed relying on a dispersion-corrected density functional theory (DFT-D) framework. The $Ln[(DPA)_n]^{(3-n)-}$ structures were stepwisely generated in silico ; the lanthanide cation was replaced by yttrium (Y^{3+}), a legitimate procedure[1] since no direct coordination with the metallic cation comes into play. Full geometry optimizations were performed using the Gaussian09 series of programs.[2] The long-range corrected Head-Gordon's ωB97X-D functional[3] was used throughout, after calibration against B3LYP and MP2, which provide in turn very similar results. Calculations were performed with the D95++** basis set[4] alongside with SDD pseudopotential for Y. A continuum solvent model (IEF-PCM) was used to mimic an aqueous media in an implicit way.[5]

Atomic charges, and thus charge transfer, were estimated with the standard NPA population analysis. Complexation energies ΔE_{AM} can be computed as the difference between the energy of the complex and the sum of the isolated molecular fragments. This nevertheless leads to an overestimation of association enthalpies/energies, since one should account for a desolvation contribution as a reference. This was mimicked resorting to a microhydration procedure (see Figure S1 infra).[6]

Optimized structures

Figure S1. Optimized structures of the microhydrated (2 water molecules) for each of the cationic systems and for the $[Ln(DPA)_3]^{3-}$ trianion, on which desolvation contributions are estimated.

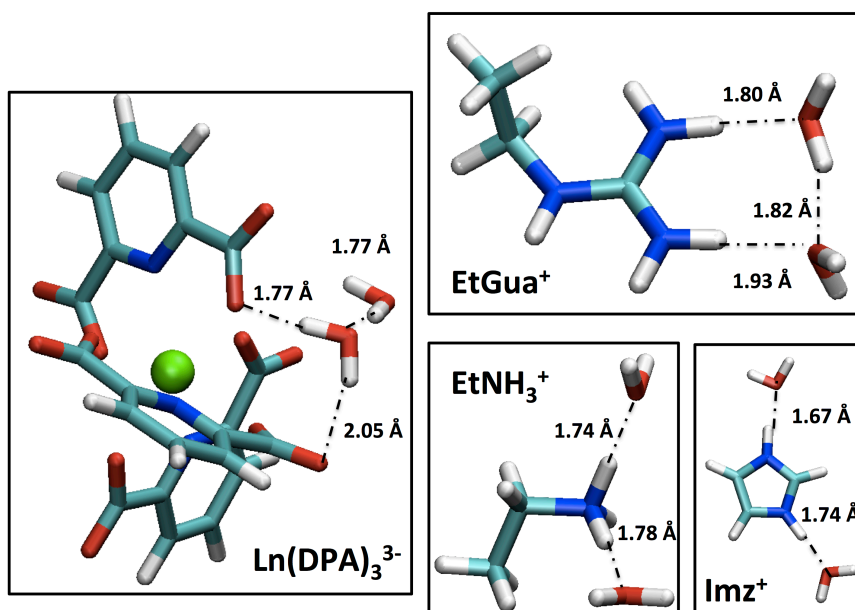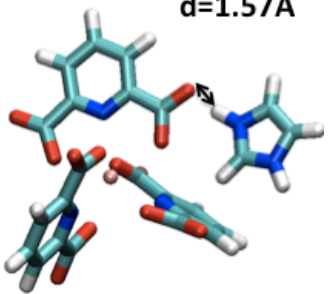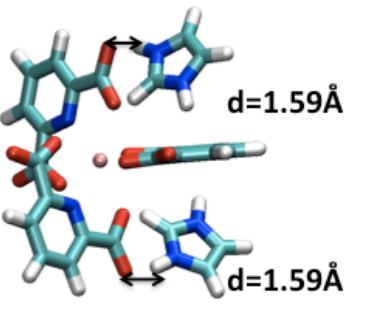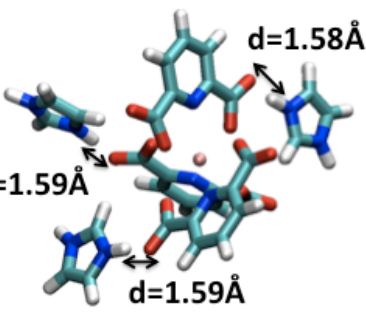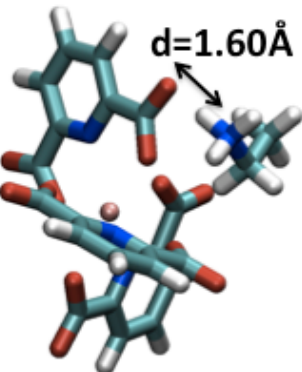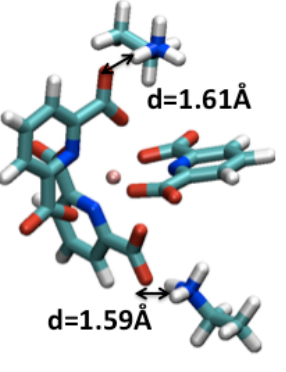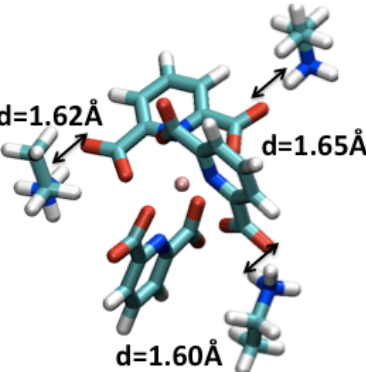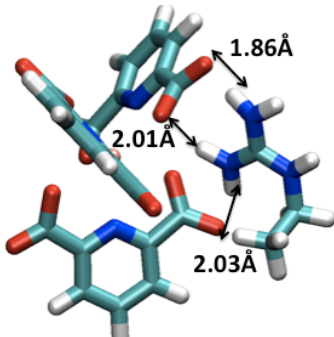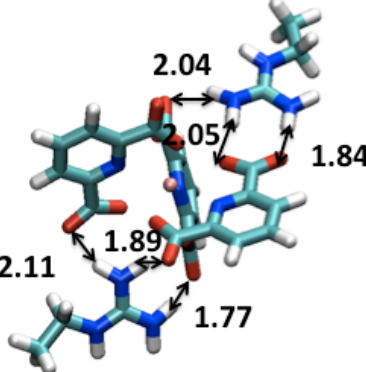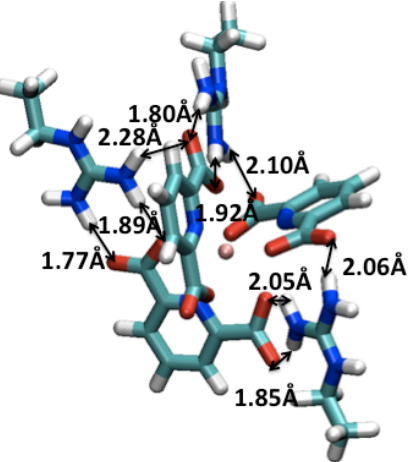**Table S2.** The nine optimized structures of the unconstrained complexes between [Tb(DPA)$_3$]$^{3-}$ and each of the A^M entities (A^M = EtGua$^+$; (b) Imz+ and (c) EtNH$_3$$^+$) that were obtained using density functional theory (DFT) calculations. Electronic and free energies are given in kcal.mol^{-1}, hydrogen bond distances (HB) are reported in Å. The charge transfer is evaluated by a natural population analysis (NPA).

[Ln(DPA)$_3$:Imz]$^{2-}$	[Ln(DPA)$_3$:Imz$_2$]$^-$	[Ln(DPA)$_3$:Imz$_3$]
ΔE^1(A^M)= 4.6 ; ΔG^1(A^M)= 1.5	ΔE^2(A^M)= 9.1 ; ΔG^2(A^M)=2.8	ΔE^3(A^M)= 10.2 ; ΔG^3(A^M)=4.1
HB network: 1.57	HB network : 1.59, 1.59	HB network : 1.58, 1.59, 1.59
Charge transfer: Δq=0.12	Charge transfer: Δq=0.24	Charge transfer: Δq=0.34
[Ln(DPA)$_3$:EtNH$_3$]$^{2-}$	**[Ln(DPA)$_3$:(EtNH$_3$)$_2$]$^-$**	**[Ln(DPA)$_3$:(EtNH$_3$)$_3$]**
ΔE^1(A^M)= 8.0 ; ΔG^1(A^M)= 2.1	ΔE^2(A^M)= 13.7; ΔG^2(A^M)= 3.9	ΔE^3(A^M)= 17.4 ; ΔG^3(A^M)=5.5
HB network : 1.60	HB network : 1.59, 1.61	HB network : 1.60, 1,62, 1,65
Charge transfer: Δq=0.10	Charge transfer: Δq=0.21	Charge transfer: Δq=0.26
[Ln(DPA)$_3$:EtGua]$^{2-}$	**[Ln(DPA)$_3$:EtGua$_2$]$^-$**	**[Ln(DPA)$_3$:EtGua$_3$]**
ΔE^1(A^M)= 10.1 ; ΔG^1(A^M)= 3.8	ΔE^2(A^M)= 17.4; ΔG^2(A^M)= 6.9	ΔE^3(A^M)= 23.3; ΔG^3(A^M)=9.4
HBs : 1.86, 2.01, 2.03	HBs: 1,77, 1.89, 2.11 ; 1.84, 2.04, 2.05	HBs: 1,77,1.89, 2.11 ; 1.80, 1.92, 2.10 ; 1.85, 2.05, 2.08
Charge transfer: Δq=0.10	Charge transfer: Δq=0.20	Charge transfer: Δq=0.29
Out-of-plane deformation φ=8°		

NMR Data

Figure S3. Experimental changes in ^{1}H NMR spectrum with increasing $\mathbf{A^M}$ equivalents (a) ethylguanidinium, (b) imidazolium, and (c) ethylammonium (n_{eq} = [$\mathbf{A^M}$] / [$Cs_3[Tb(DPA)_3]$]), in a solution of $Cs_3[Tb(DPA)_3]\cdot 7H_2O$ (solvent: D_2O; proton resonance frequency: 200 MHz; T = 298 K; C_0 = (a) 15.5 mol.L^{-1}, (b) 16.2 mol.L^{-1} and (c) 16.2 mol.L^{-1}). Protons labeling refers to the assignment that is indicated on the ammonium structures displayed in Figure 1.
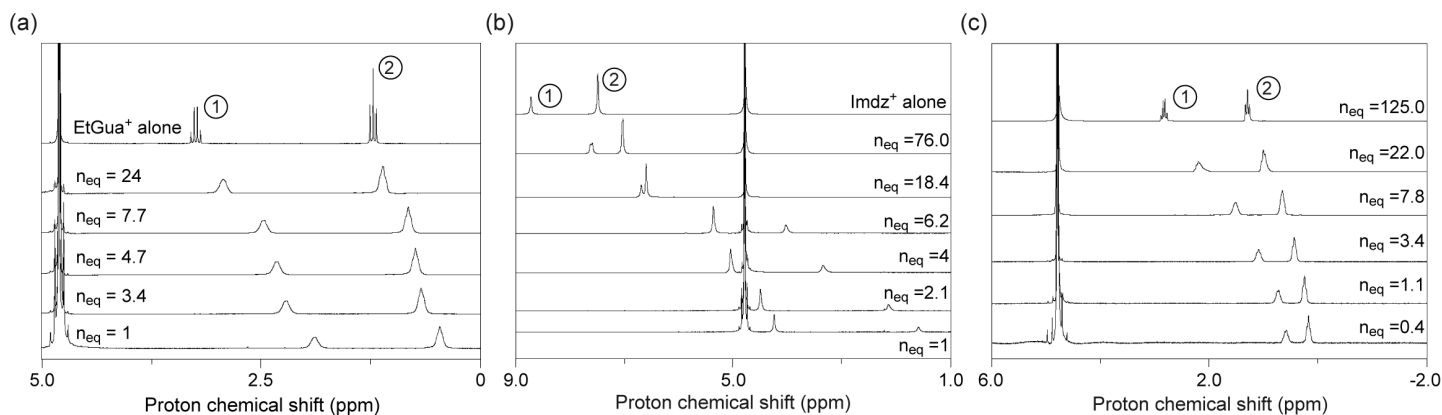

Figure S4. The intersections of the {K_1, K_2, K_3} distributions that have been determined, using an enhanced "coarse grid search" protocol, from the NMR titration curves that were recorded for EtGua$^+$, EtNH$_3$$^+$ and Imz$^+$. The best fit for each $\mathbf{A^M}$ is indicated with plain lines. The shift measuring accuracy is assumed to be mainly limited by the width of the probed proton signals, and has been estimated in a range between 0.03 and 0.06 ppm for each data set.
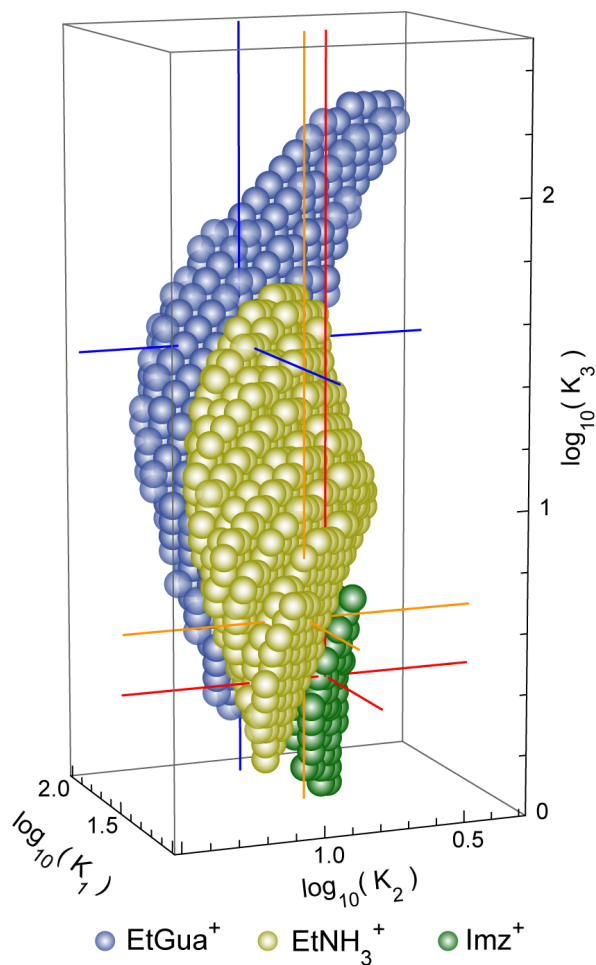
References

1. A. Bourdolle, M. Allali, J. C. Mulatier, B. Le Guennic, J. M. Zwier, P. L. Baldeck, J. C. G. Bunzli, C. Andraud, L. Lamarque and O. Maury, *Inorg. Chem.*, 2011, **50**, 4987-4999.

2. M. J. Frisch, G. W. Trucks, H. B. Schlegel, G. E. Scuseria, M. A. Robb, J. R. Cheeseman, G. Scalmani, V. Barone, B. Mennucci, G. A. Petersson, H. Nakatsuji, M. Caricato, X. Li, H. P. Hratchian, A. F. Izmaylov, J. Bloino, G. Zheng, J. L. Sonnenberg, M. Hada, M. Ehara, K. Toyota, R. Fukuda, J. Hasegawa, M. Ishida, T. Nakajima, Y. Honda, O. Kitao, H. Nakai, T. Vreven, J. Montgomery, J. A.;, J. E. Peralta, F. Ogliaro, M. Bearpark, J. J. Heyd, E. Brothers, K. N. Kudin, V. N. Staroverov, R. Kobayashi, J. Normand, K. Raghavachari, A. Rendell, J. C. Burant, S. S. Iyengar, J. Tomasi, M. Cossi, N. Rega, J. M. Millam, M. Klene, J. E. Knox, J. B. Cross, V. Bakken, C. Adamo, J. Jaramillo, R. Gomperts, R. E. Stratmann, O. Yazyev, A. J. Austin, R. Cammi, C. Pomelli, J. W. Ochterski, R. L. Martin, K. Morokuma, V. G. Zakrzewski, G. A. Voth, P. Salvador, J. J. Dannenberg, S. Dapprich, A. D. Daniels, Ö. Farkas, J. B. Foresman, J. V. Ortiz, J. Cioslowski and D. J. Fox, Gaussian, Inc., Wallingford CT, 2009.

3. J. D. Chai and M. Head-Gordon, *Phys. Chem. Chem. Phys.*, 2008, **10**, 6615-6620.

4. T. H. J. Dunning and P. J. Hay, ed. H. F. S. III, Plenum, New York, 1976, vol. 3, pp. 1-28.

5. J. Tomasi, B. Mennucci and R. Cammi, *Chem. Rev.*, 2005, **105**, 2999-3093.

6. D. Jacquemin, C. Michaux, E. A. Perpete and G. Frison, *J. Phys. Chem. B*, 2011, **115**, 3604-3613.